



Study of water in Ca-montmorillonite by thermal analysis and positron annihilation lifetime spectroscopy

Igor Mat'ko¹ · Ondrej Šauša¹ · Katarína Čechová¹ · Karol Jesenák²

Received: 11 August 2017 / Accepted: 27 February 2018 / Published online: 12 March 2018
© Akadémiai Kiadó, Budapest, Hungary 2018

Abstract

The aim of this study is to characterize adsorbed liquid in montmorillonite structure for different levels of adsorption by both thermoanalytical and microstructural methods. Montmorillonite of Ca type is used for the analysis. Water desorption process occurring typically between 50 and 180 °C is analysed in details by thermogravimetric analysis. Thermal response of adsorbed water for the selected steps of desorption process is studied by differential scanning calorimetry. Corresponding characterization of free volume is performed by positron annihilation lifetime spectroscopy. An attempt to determine a correlation of characterization method results is provided.

Keywords Montmorillonite · Thermogravimetric analysis · DSC · Positron annihilation lifetime spectroscopy

Introduction

Montmorillonite is a microcrystalline mineral from the group of phyllosilicates and belongs in nature among the most widespread minerals. It has an extremely wide use in various industries, for example as catalytic processes agent, desiccant to remove moisture, inorganic filler in the polymer industry [1, 2]. Most of its applications use its unique sorption and colloidal properties. Chemically, it is hydrated sodium calcium aluminium magnesium silicate hydroxide $(\text{Na,Ca})_{0.33}(\text{Al,Mg})_2(\text{Si}_4\text{O}_{10})(\text{OH})_2 \cdot n\text{H}_2\text{O}$; exact ratio of cations varies with source.

Particular feature of montmorillonite is its rather complex porous structure. It is formed by layered sheet particles of average diameter ~ 500 nm and thickness of ~ 1.0 nm with specific inner and outer surface which is characterized by enhanced cation exchange capacity. Such a structure contains rather high amount of interlayer space. Water and other polar liquids are highly adsorbed by the

surface of montmorillonite particles. As the liquid can penetrate to interlayer space, montmorillonite structure swells. The amount of expansion is due largely to the type of exchangeable cation contained in the structure. In certain cases, the material can increase its volume several times.

The liquid adsorbed by porous structure finds itself in so-called confined state. Various studies of the systems porous structure-adsorbed liquid have revealed that numerous physical properties of such confined liquids and probably also solids might be modified or even principally changed [3–7]. The variability of thermal and mechanical properties of such systems still needs to be investigated. Moreover, the water itself represents a liquid with relatively complex thermal behaviour and merits further analysis of the influence of confined state on its physical properties.

Recently, systematic research of confined systems associating differential scanning calorimetry (DSC) and positron annihilation lifetime spectroscopy (PALS) methods has been launched [6–11]. DSC is the principal thermoanalytical method which, by measuring the enthalpy evolved or adsorbed by the investigated sample, can specify the change of the sample's thermodynamic state, namely the onset and minimum peak temperatures and the heat of the solidification or of the melting of studied material. Useful supporting technique is thermogravimetric

✉ Igor Mat'ko
igor.matko@savba.sk

¹ Institute of Physics, Slovak Academy of Sciences, Dúbravská 9, 845 11 Bratislava, Slovakia

² Department of Inorganic Chemistry, Faculty of Natural Sciences, Comenius University, Mlynská dolina CH-2, 842 15 Bratislava, Slovakia

analysis (TG) in which the mass of sample is measured during thermally induced sample transformation. PALS is a suitable technique for the study of confined systems via the free-volume approach. It is based on the measurement of lifetime of positron or positronium (Ps, bonded state of electron and positron) in the matter. This technique allows to determine the free-volume void sizes as well as their temperature dependence from the measured ortho-positronium (Ps in the triplet state) lifetime. The lifetimes $\tau_{o\text{-Ps}}$ in the sample can be converted most frequently into the radii of the free-volume voids R_h using a semi-empirical quantum mechanical model of o-Ps in a spherical void by the equation [12, 13]:

$$\tau_{o\text{-Ps}} = 0.5 \left[1 - (R_h / (R_h + \Delta R)) + (2\pi)^{-1} \sin(2\pi R_h / (R_h + \Delta R)) \right]^{-1}, \quad (1)$$

where $\Delta R = 0.1656$ nm is an empirical parameter. This correlation is valid and commonly used for the o-Ps lifetimes in solids and lowers than 10 ns. More complicated relations for other pore geometry, large pores as well as excited energy levels are included in the EELViS routine for the estimation of pore sizes from the o-Ps lifetime [14]. However, we must note that in the case of liquids the bubble effect occurs at the formation of Ps [15, 16], and the free volume “seen” by Ps at its localization place is greater than real intermolecular space in liquids measured by other methods.

The theme of water interaction and montmorillonite is a subject of long-term wide research [17], but studies using combination of thermal and microstructural characterization, namely by PALS, are rather rare. This work deals with properties of water in Ca-montmorillonite. The choice of calcium montmorillonite was influenced by the fact that calcium ions are most often represented in the variable positions of the montmorillonite. However, natural montmorillonites typically do not contain only one ion type in these positions. For better characterization of our montmorillonite, the original form of montmorillonite was converted to a monionic calcium form. Further an attempt to correlate the analysis with microstructural data obtained via free-volume approach is presented. The study is a part of complex investigation of the structure and properties of confined nanosystems [6–11].

Materials and methods

Montmorillonite was isolated by decanting method from 4% water suspension of bentonite from deposit of Stará Kremnička–Jeľšovský potok (Slovak Republic) [18]. Ca^{2+} -doped montmorillonite was prepared by ion-exchange reaction in the water solution of CaCl_2 (concentration

$c_{\text{sol}} = 0.2$ mol dm^{-3}) using five repeated cycles. Montmorillonite doped in this way was washed by distilled water and dried in vacuum. More detailed information on bentonite and montmorillonite from this site is given elsewhere [19, 20].

Microstructural and chemical analysis was carried out using JEOL JSM 6610 scanning electron microscope (SEM) operated at 15 kV and equipped with energy-dispersive spectroscopy detector (EDX) (Oxford Instruments).

Anhydrous montmorillonite was prepared by drying for 24 h at 393 K (120 °C) in a vacuum of 10^{-6} mbar. Samples from this material for desorption experiments were closed for at least 24 h in a water vapour container to prepare samples in fully saturated state. The pure water LC-MS Ultra CHROMASOLV from Honeywell/Riedel-de Haen was used.

The TG analysis measurements were taken using TGA7 (PerkinElmer) in both linear heating and isothermal regimes using dynamic argon atmosphere. For isothermal analysis, the sample was kept at temperature $T_{\text{an}} = 323$ K (30 °C) for 600 min. Linear heating measurements were taken in temperature region 303–453 K (30.0–180.0 °C) with the rates $w = 1.0, 2.0, 5.0$ and 10.0 K min^{-1} . Mass loss coefficient m_1 , which determines the mass loss of the sample during measurements, can be directly determined from relative mass coefficient k measured by TG unit as $m_1 = 1 - k$.

DSC measurements were taken using power-compensation DSC8500 (PerkinElmer) with automatic intracooler (200 K). Samples of 15–30 mg encapsulated in air and measured in dynamic nitrogen atmosphere were used. Both hermetic and non-hermetic encapsulation was used for specific way of study of thermal properties. For certain analyses, the samples of material after specific pre-treatment by TG were analysed.

Continuous cooling and heating regimes with the rates of $w = -2.0$ or $+2.0$ K min^{-1} , respectively, were applied. Each DSC measuring cycle started at 303.0 K, and the cool/heat procedure was used. It means that firstly each sample was slowly cooled to 213.0 K; a temperature which is sufficiently below the equilibrium crystallization temperature of water and the solidification was measured; then, it was continuously heated up to 303.0 K and the corresponding melt transition was detected.

Positron annihilation lifetime spectra were measured by the conventional fast–fast coincidence time spectrometer with the time resolution about 320 ps FWHM determined using Al defect-free sample. LT programme [21] was used for the analysis of spectra. Three lifetime components were fitted during the analysis. Shorter lifetimes τ_1 and τ_2 (in subnanosecond range) are connected with the annihilation of para-positronium and free positrons. Larger lifetime τ_3 (in nanosecond range) originated from the annihilation of

ortho-positronium in free volumes of different sizes is important for this study and was discussed later. The correction on the positron annihilation in the source as well as in the sample container kapton foil window was taken into account.

The amount of water in the montmorillonite matrix for samples analysed by PALS was determined by weighing. The partial mass of water (or coefficient of filling) in each measured sample is defined as:

$$c = \frac{m_{\text{H}_2\text{O}}}{m_{\text{MMT}}}, \quad (2)$$

where $m_{\text{H}_2\text{O}}$ and m_{MMT} are mass of water and pure montmorillonite ($\pm 0.1\%$), respectively, in the prepared sample. Lower c values were achieved by evaporating the water from the matrix; very low c values are obtained by short evaporation in a weak vacuum.

Results and discussion

Conventional SEM analysis of montmorillonite samples microstructure revealed rather broad particle size distribution which is in principal agreement with previous detailed analysis [19] (Fig. 1a). Chemical analysis by EDX detected no presence of Na, which was one of exchange cations in original form of studied montmorillonite (Fig. 1b). The presence of Mg at place of exchange cations cannot be excluded by this method as it is present also in silicate layers as a aluminium substituent. However, results of this analysis allow to assume that studied material was successfully converted by ion-exchange reaction to calcium form.

The solid–liquid phase transition for full vapour adsorption filling of Ca-montmorillonite (as-prepared sample) was examined by calorimetric measurements. The sequence of two cycles (the cooling and heating runs) immediately after each other was realized in the DSC to verify the reproducibility of each individual transformation step (Fig. 2). Characteristic DSC curve exhibits hysteretic behaviour, i.e. crystallization in the pores is detected at lower temperatures compared to melting; such a thermal behaviour of water confined in porous structures had been observed by many previous studies [3]. Contrary to typical curves obtained in these studies, not only solidification peak but also melting peak finds itself well below 0 °C (273.15 K), e.g. below melting temperature of bulk water. This result can be explained by the fact that all water (giving thermal response) adsorbed by the montmorillonite structure finds itself in confined state, where it is under the pressure generated by montmorillonite structure swelling. Corresponding shift of transformation temperature, denoted as melting or solidification point depression, is the

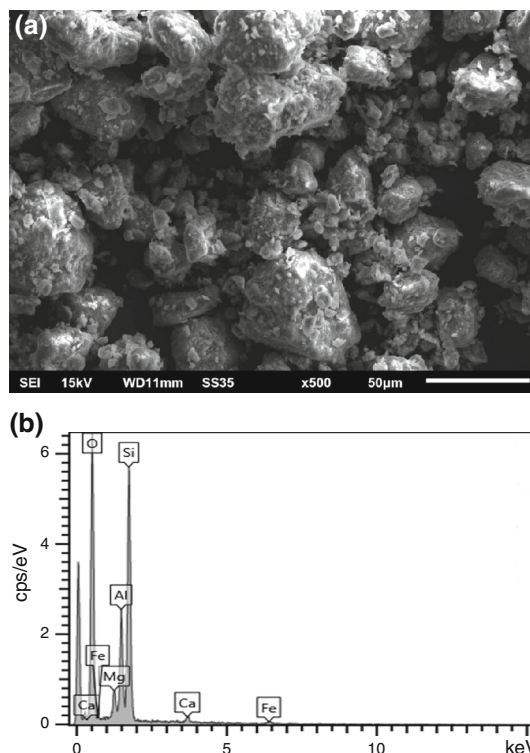


Fig. 1 a SEM micrograph of studied Ca-montmorillonite structure. b EDX analysis showing chemical composition

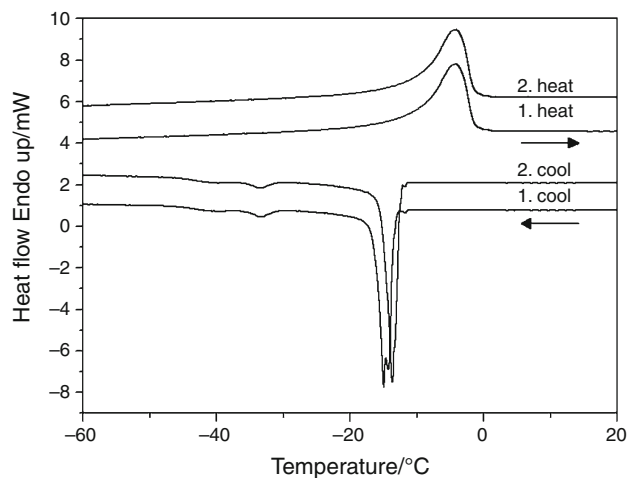


Fig. 2 DSC curve of hermetically encapsulated sample of water-filled Ca-montmorillonite in as-prepared state showing two cooling/heating cycles, rate $w = 2 \text{ K min}^{-1}$

consequence of Gibbs–Thompson law [22]. Especially for the cooling regime rather complex thermal response is evident (Fig. 2). Rather intensive peak of low reproducibility with onset temperature $\sim -12.0 \text{ }^\circ\text{C}$ ($\sim 261.0 \text{ K}$) is followed by two tiny peaks of high reproducibility with onset temperatures $\sim -32.0 \text{ }^\circ\text{C}$ ($\sim 241.0 \text{ K}$) and $\sim -39.0 \text{ }^\circ\text{C}$ ($\sim 234.0 \text{ K}$),

respectively. A fine structure of the intensive peak is evident. This feature can be interpreted by the fact that it represents a convolution of several fine peaks (located in the interval ~ -12.0 to -16.0 °C) corresponding to the solidification of various parts of confined water finding itself under local pressure of various value. The local pressure distribution changes during solidification–melting cycles, what causes the observed low reproducibility of the corresponding peak.

The occurrence of tiny peak at ~ -41.0 °C (~ 232.0 K) is typically observed during DSC analysis of confined water-containing systems. This peak is ascribed to the crystallization of confined water in the spherical cavities by homogenous nucleation [23, 24]. Its presence shows that some part of confined water in montmorillonite structure finds itself in regions where it is isolated from ice front percolation during solidification. The consequence is that it can be supercooled down to the temperature, which is considered as a lowest attainable temperature for pure water when crystallization by homogeneous nucleation occurs [25].

This effect is more complex for montmorillonite than for previously studied confined water-containing systems [11]. It manifests itself by the presence of two peaks of slightly different intensity with onset temperatures ~ -32.0 °C (~ 241.0 K) and ~ -39.0 °C (~ 234.0 K), respectively. This is probably related to specificity of montmorillonite pores structure; however, the interpretation is still open. This effect is relatively more pronounced as well, the area of corresponding peaks represents more than 8% total area of solidification peaks, while, e.g. for controlled pore glass, CPG126 was that almost negligible ($< 0.1\%$) [11]. Besides good reproducibility, these two peaks exhibit one more specific feature which will be explained later.

The adsorbed water was further analysed in combination with TG analysis. TG measurements were taken in temperature region 30.0–180.0 °C (303–453 K). This temperature region corresponds to the complete loss of water adsorbed in the montmorillonite structure, dehydration caused a mass loss of approximately 25% ($m_1 = 0.25$) (Fig. 3a). Detailed analysis of TG curve revealed that this process consists of three apparent steps as the curve derivative exhibits three identifiable peaks. This result is in principal accord with previous DTA studies of montmorillonite. Numerous papers had shown that for +2 cations the dehydration process corresponds to double or triple peak [26]. For a threefold dehydration peak, it is presumed that first the moisture adsorbed on the surface is released, followed by the water molecules bound to the +2 exchanged cations and lastly the molecules bound to the tetrahedral layer of the montmorillonite structure.

Typical temperatures for individual steps (corresponding to maximum of derivative peaks) were estimated as

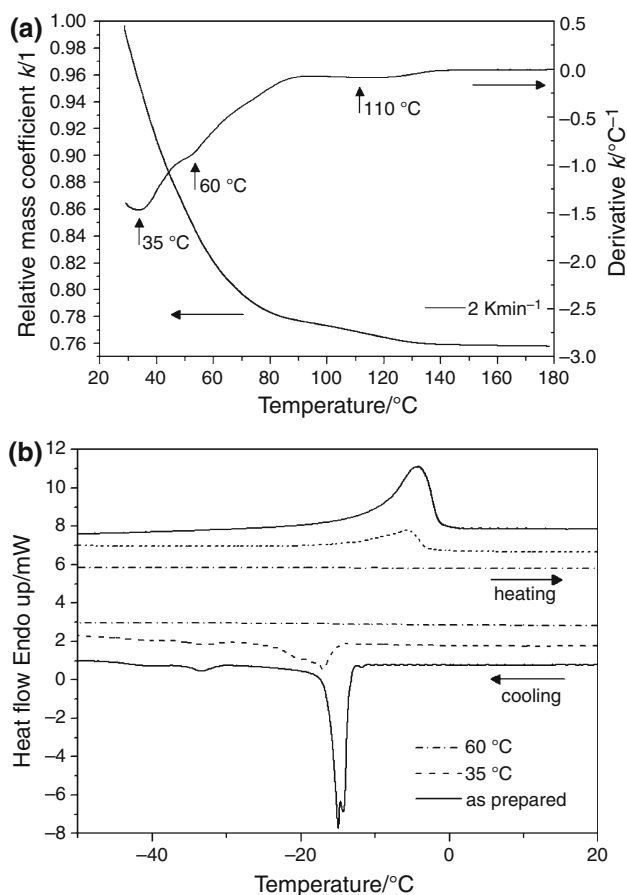


Fig. 3 **a** TG analysis of sample, heating rate $w = 2 \text{ K min}^{-1}$. **b** DSC curves of hermetically encapsulated samples of water-filled Camontmorillonite after treatment by TG (cooling/heating rate $w = 2 \text{ K min}^{-1}$). The selected temperatures are marked in **(a)**. The curve of as-prepared sample is shown for comparison (curve of sample heated to 110 °C is not shown as it gives the result identical to that of 60 °C)

$T_1 = 35$ °C (308 K), $T_2 = 60$ °C (333 K) and $T_3 = 110$ °C (383 K); the values were determined for the heating rate of $w = 2.0 \text{ K min}^{-1}$ (Fig. 3a). Corresponding mass losses were determined as $m_{11} = 5.4\%$, $m_{12} = 17.9\%$ and $m_{13} = 22.7\%$, respectively. Three samples were prepared in these states by initial heating in TG unit to corresponding temperature after which the sample was immediately hermetically encapsulated and analysed by DSC. The results of their analyses were compared with that of as-prepared sample (Fig. 3b). From the results, it is evident that a significant part of the water giving a thermal response during DSC analysis is released during the first step of dehydration. Its complex nature seems to be conserved during releasing. This part of adsorbed water represents only its small fraction and is rapidly released from montmorillonite pores. Heating of sample to temperature T_1 causes the loss of approximately only one tenth of its total amount (entire loss after heating to 180 °C is $\sim 25\%$), but

already almost two-thirds of this part are released as can be estimated from the corresponding DSC peak areas.

In order to obtain more punctual data on this step, an isothermal analysis was carried out using both TG and DSC techniques. A non-hermetically encapsulated sample of studied material in as-prepared state was analysed by DSC using the series of analogical measurements, e.g. the cooling and heating runs (cooling/heating rate $w = \pm 2.0 \text{ K min}^{-1}$). The sample was kept between individual runs at $30 \text{ }^\circ\text{C}$ for 5 min. A systematic decrease in DSC peak areas is observed (Fig. 4a); the first peak (which is in fact the convolution of several fine peaks with original onset temperature $\sim -12.0 \text{ }^\circ\text{C}$) disappears after seven cycles when it joins the first of tiny low-temperature peaks (with onset temperature $\sim -32.0 \text{ }^\circ\text{C}$). This time interval corresponds to total time of sample annealing at $30 \text{ }^\circ\text{C}$ to 35 min approximately. The low-temperature peaks

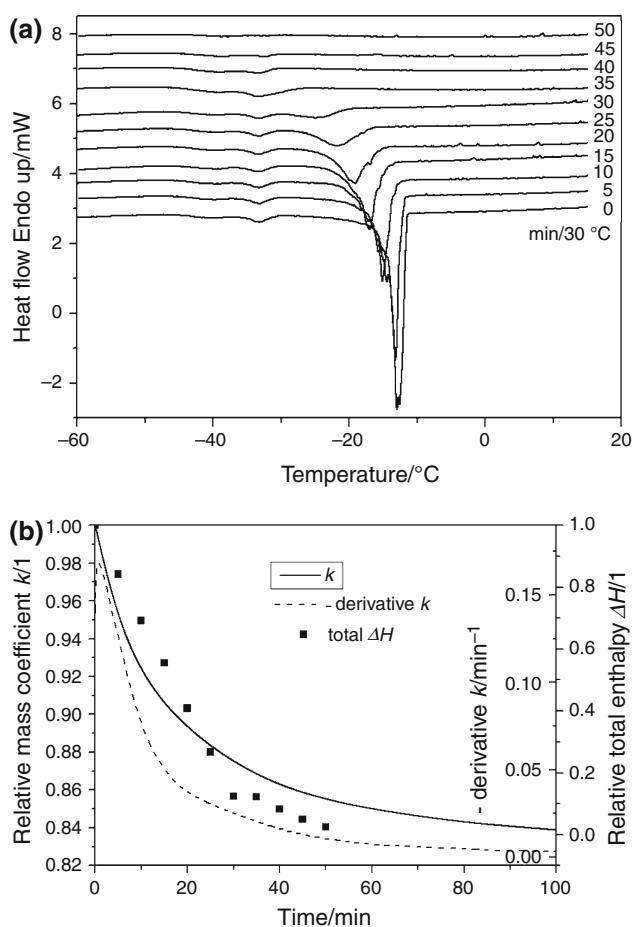


Fig. 4 **a** DSC curve of non-hermetically encapsulated sample of water-filled Ca-montmorillonite, cooling rate $w = 2 \text{ K min}^{-1}$. The sample was kept at $30 \text{ }^\circ\text{C}$ for 5 min between individual cooling–heating cycles. Only cooling curves are shown for clarity. **b** TG analysis of sample by annealing at $30 \text{ }^\circ\text{C}$. The total enthalpy evolution ΔH determined from (a) is shown for comparison (in relative values)

disappear after next three cycles, e.g. after total time of sample annealing at $30 \text{ }^\circ\text{C}$ approximately 50 min. The joining of peaks occurs because of specific phenomenon, namely shift of first solidification peak towards lower temperatures with decreasing water content. An analogous feature was already observed during studies of confined water-containing systems. An attempt of its interpretation is based on blocking mechanism on ice front percolation during water solidification [11]. It has to be noted that low-temperature peaks do not shift during all thermal cycles of this analysis and do not decrease their areas during the first six cycles. This fact supports the assumption that they correspond to solidification by homogenous nucleation.

Analogous characterization was done by the TG analysis of sample by annealing at $30 \text{ }^\circ\text{C}$ (Fig. 4b). Total area of DSC solidification peaks is compared with corresponding TG curve. Derivative of TG curve shows several steps of its evolution. Similarity with solidification peaks area evolution allows assume that first two steps correspond to the release of corresponding forms of adsorbed water. Using this assumption, one can estimate that loosening of corresponding part of adsorbed water (giving thermal response in DSC) was finished roughly after 45–50 min.; the sample lost $\sim 14\text{--}15.0\%$ of its mass during this time (which is $\sim 60\%$ of total amount adsorbed water). Using this coefficient for the estimation of corresponding mass of water in hermetically encapsulated sample analysed by DSC (Fig. 2), one obtain total enthalpy of solidification for 1.cooling run $260.2\text{--}278.8 \text{ J g}^{-1}$ and total enthalpy of melting for 1.heating run $286.8\text{--}307.3 \text{ J g}^{-1}$. An analogous discrepancy between enthalpy values for cooling and heating runs as well as deficit to table data of that for pure water (333.6 J g^{-1}) had been obtained for previous studies of confined water-containing systems [11]. The discrepancy seems to be a specificity of the used method of thermal analysis of water (it was observed even for pure water). For the observed deficit to table data, it had been supposed that it had confirmed an existence of certain part of water that does not crystallize during solidification. However, in this case such an interpretation is problematic. It has to be noted that the used estimation is loaded with a certain error as the evaporation rates are not necessarily the same in the DSC and TG units. Moreover, there is obviously an overlapping with the second step of dehydration (corresponding to the release of water molecules bound to the + 2 exchanged cations) as the material was continuously losing its mass in the course of annealing, e.g. for 600 min., it lost 17.8% of its mass.

Because the rate of dehydration strictly depends on the heating rate, its process steps shift to higher temperatures increasing its value. TG analysis using various heating rates, namely $w = 1.0, 2.0, 5.0$ and 10.0 K min^{-1} , was carried out (Fig. 5). From the derivative of corresponding

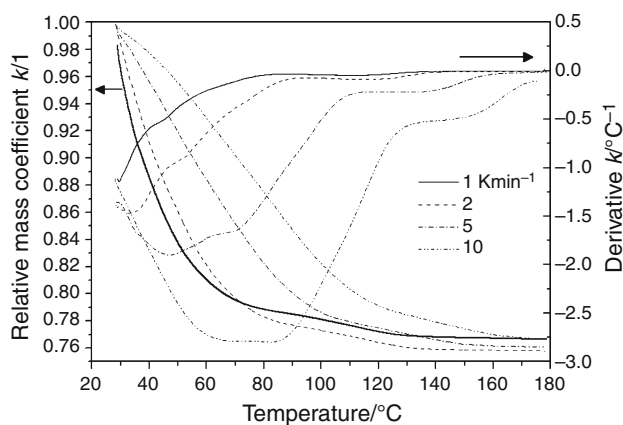


Fig. 5 TG analysis of sample heating rates $w = 1.0, 2.0, 5.0$ and 10.0 K min^{-1}

TG curves, the activation energies of individual steps were determined by the use of the Kissinger method [27], namely $E_1^* = 217 \pm 122 \text{ J mol}^{-1}$, $E_2^* = 724 \pm 70 \text{ J mol}^{-1}$ and $E_3^* = 6087 \pm 1097 \text{ J mol}^{-1}$, respectively. It has to be noted that these values are loaded with a significant error and have only indicative meaning. It is because of high overlapping of dehydration process step peaks on derivatives of TG curves, and for this reason, it is difficult to determine their exact positions. Relatively low values of E_a^* correspond well to several levels of physisorption, e.g. only weak bonding of water molecules to montmorillonite structure and are in good agreement with usually accepted model of three forms of water molecules bonding in montmorillonite [26].

The o-Ps lifetime (as the third and longest lifetime spectrum component, τ_3) depending on the water content (in the range 0–0.4 of c values) at the temperature $T = 298 \text{ K}$ in the montmorillonite matrix is shown in Fig. 6. Since the pores in montmorillonite are bounded by parallel layers, we can estimate the interlayer spacing l from τ_3 for coefficient of filling $c = 0$ by using the parallel plate model [14]. For $\tau_3 = 6.2 \text{ ns}$, we obtained the value $l = 0.57 \text{ nm}$, which is in good agreement with 0.56 nm from XRD measurements for Ca-montmorillonite [28]. Because the o-Ps lifetime τ_3 is proportional to the size of the free space where o-Ps is annihilated, τ_3 reflects the reduction of the free space between molecules in interlayer gap gradually as the free space between silicate layers is filled with water molecules. This free space can be approximated by sphere, and the free-volume size can be estimated by Eq. (1). In the dependence $\tau_3(c)$ in the range c of 0.15–0.36, we can see no significant deviations from the linear trend. From $c = 0.36$ and above, τ_3 does not change and is close to the value of 1.8 ns for liquid water [29].

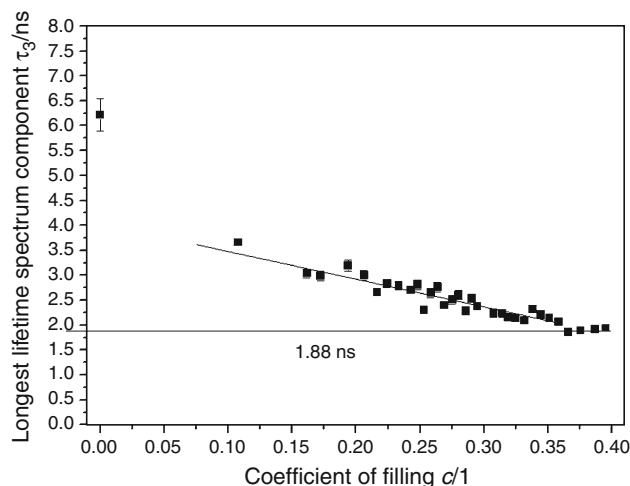


Fig. 6 PALS analysis of water-filled montmorillonite. Dependence of longest lifetime spectrum component, τ_3 , on water amount c

The formation of Ps in montmorillonite is small, as shown by other measurements [28]. Intensity I_3 is less than 2% for all measured values. It increases from 0.8 to 2% as the water content increases.

To correlate the results of PALS measurements with TG analysis, we first remind that relative mass coefficient k , measured by TG unit, is defined as:

$$k = \frac{m_{\text{H}_2\text{O}} + m_{\text{MMT}}}{m_{\text{H}_2\text{O}} + m_{\text{MMT}}}, \quad (3)$$

where $m_{\text{H}_2\text{O}}$ and m_{MMT} are mass of water and pure montmorillonite, respectively, in the analysed sample. The $m_{\text{H}_2\text{O}}$ represents initial mass of adsorbed water (supposed to correspond to maximal amount of adsorbed water or saturation state). It can be shown that mass loss coefficient m_l , which can be directly determined from normalized mass coefficient k , is related to coefficient of filling defined by (2) as:

$$m_l = \frac{c_s - c}{c_s + 1}, \quad (4)$$

where $c_s = m_{\text{H}_2\text{O}}/m_{\text{MMT}}$ means the coefficient of filling in saturation, i.e. coefficient of filling for maximal amount of water adsorbed by montmorillonite (using sample preparation by vapour adsorption). To determine its exact value is tricky task and encounters a problem of slight discrepancy between TG results and water amount determination by weighing for PALS analysis. Supposing the maximal value determined during PALS sample preparation $c_s = 0.4$, the corresponding maximal mass loss (when $c = 0$) should be $m_{ls} = 0.286$ (28.6%). Such a high value was never attained by TG analysis. For typically observed mass loss values $\sim 25\%$ the coefficient of filling in saturation should be ~ 0.35 which is close to the value when the value of lifetime spectrum component τ_3 achieves that

of liquid water (Fig. 6). The discrepancy could be understood if we suppose that the excess of water over $c = 0.35$ represents a moisture on the surface of montmorillonite particles which can be detected only for relatively larger amounts of material used for PALS samples (~ 1 g). This part of water represents in fact bulk water. It is very quickly released from the studied material during preparation of significantly smaller samples for thermal analysis and finally has no contribution to the results. It has to be noted again that all water giving thermal response during cooling–heating treatment of material by DSC should be under the pressure generated by montmorillonite structure swelling because of melting point depression (Fig. 2). Generally, the quick evaporation of the adsorbed water at the beginning must be a reason of doubtful definition of the initial state of sample analysed by TG which causes a slight discrepancy of total mass loss between individual experiments ($\sim 1\%$) (Fig. 5). Using this interpretation, the first step of dehydration, i.e. the concentration range when the water giving thermal response is present in the sample, corresponds to the region of slower linear increase in lifetime spectrum component τ_3 from the value close to that of liquid water to ~ 3.0 ns.

Conclusions

According to TG study dehydration of water-adsorbed Ca-montmorillonite (elaborated by vapour adsorption process) takes place in three apparent steps. The material loses $> 25\%$ of its original mass. This result is in principal agreement with the usually observed thermal behaviour of analogous form of montmorillonite.

A significant part of water giving a thermal response during cooling–heating treatment of material by DSC is released during the first step of dehydration. Its thermal behaviour is rather similar to that of confined water in other fine porous structures. The solidification of this part of water consists mainly of heterogeneous nucleation, the onset temperature of which depends on water content. Relatively important fraction of this part exhibits homogeneous nucleation with constant onset temperature ~ -32.0 °C (~ 241.0 K). The release of this part is finished after the release of $\sim 60\%$ of total amount adsorbed water.

The following two steps of dehydration correspond well to usually accepted model of three forms of water molecules bonding in montmorillonite, e.g. water molecules bonded to exchangeable cations and water molecules bonded to layers of the structure.

PALS measurements showed that for the water content in the range of concentration values ~ 0.15 – 0.36 , which corresponds to the concentration range when water giving

thermal response in DSC (released during first step of dehydration) is present in the structure, the longest lifetime spectrum component τ_3 linearly decreases from 3.0 to 1.8 ns which is the value close to that of liquid water. Interlayer spacing of Ca-montmorillonite without water ($c = 0$) determined from corresponding lifetime spectrum component τ_3 value (using parallel plate model) is in good agreement with the value determined by other structural methods.

Obviously further research is essential to understand more aspect of really complex thermal behaviour of this type confined water system.

Acknowledgements Work was partially supported by projects VEGA 2/0127/17, VEGA 2/0157/17, APVV-16-0369 and APVV-15-0621.

References

- Kader MA, Kim K, Lee Y-S, Nah C. Preparation and properties of nitrile rubber/montmorillonite nanocomposites via latex blending. *J Mater Sci.* 2006;41:7341–52.
- Lloyd L. Handbook of industrial catalysts. New York: Springer; 2011.
- Riikonen J, Salonen J, Lehto VP. Utilising thermoporometry to obtain new insights into nanostructured materials: review part 1. *J Therm Anal Calorim.* 2011;105:811–21.
- Riikonen J, Salonen J, Lehto VP. Utilising thermoporometry to obtain new insights into nanostructured materials: review part 2. *J Therm Anal Calorim.* 2011;105:823–30.
- Landry MR. Thermoporometry by differential scanning calorimetry: experimental considerations and applications. *Thermochim Acta.* 2005;433:27–50.
- Illeková E, Miklošovičová M, Šauša O, Berek D. Solidification and melting of cetane confined in the nanopores of silica gel. *J Therm Anal Calorim.* 2012;108:497–503.
- Illeková E, Krištiak J, Macová E, Mat'ko I, Šauša O. Rearrangement of hexadecane molecules confined in the nanopores of a controlled I pore glass using positron annihilation and differential scanning calorimetry. *J Therm Anal Calorim.* 2013;113:1187–96.
- Iskrová M, Majerník V, Illeková E, Šauša O, Berek D, Krištiak J. Free volume seen by positronium in bulk and confined molecular liquid. *Mat Sci Forum.* 2009;607:235–7.
- Šauša O, Illeková E, Krištiak J, Berek D, Macová E. PALS and DSC study of partially filled nanopores by E hexadecane. *J Phys Conf Ser.* 2013;443:012059.
- Illeková E, Macová E, Majerník V, Mat'ko I, Šauša O. Anomalous thermal expansion of thin cetane layer solidified at the inner surface of confining nanoporous silica gel. *J Therm Anal Calorim.* 2014;116:753–8.
- Mat'ko I, Šauša O, Macová E, Berek D. Combined study of confined water in controlled pore glasses by differential scanning calorimetry and positron annihilation lifetime spectroscopy. *J Therm Anal Calorim.* 2015;121:163–8.
- Tao SJ. Positronium annihilation in molecular substances. *J Chem Phys.* 1972;56:5499–510.
- Eldrup M, Lightbody D, Sherwood JN. The temperature dependence of positron lifetime in solid pivalic acid. *Chem Phys.* 1981;63:51–8.
- Zaleski, R. EELViS. <http://eelvis.sourceforge.net> (2009). Accessed 15 Jun 2011.

15. Ferrell RA. Long lifetime of positronium in liquid helium. *Phys Rev.* 1957;108:167.
16. Goworek T. Positronium as a probe of small free volumes in crystals, polymers and porous media. *Ann Univ Maria Curie-Skłodowska, Lublin-Polonia.* 2014;69:1–110.
17. González Sánchez F, Jurányi F, Gimmi T, Van Loon L, Seydel T, Unruh T. Dynamics of supercooled water in highly compacted clays studied by neutron scattering. *J Phys Condens Matter.* 2008. <https://doi.org/10.1088/0953-8984/20/41/415102>.
18. Jesenák K. Laboratory device for sedimentation separation of powders. *Ceramics.* 1994;38:35–6.
19. Jesenák K, Kuchta L, Guller L, Fúsková J. Physico-chemical properties of Bentonite “Stará Kremnička – Jelšový potok” I: particle size distribution. *Mineralia Slovaca.* 1997;29:439–42.
20. Jesenák K, Fajnor V. Distribution of trace elements in bentonite Stará Kremnička – Jelšový potok. *Mineralia Slovaca.* 1995;27:221–4.
21. Kansy J. Microcomputer program for analysis of positron annihilation lifetime spectra. *Nucl Instrum Method A.* 1996;374:235–44.
22. Brun M, Lallemand A, Quinson J, Eyraud C. A new method for simultaneous determination of size and shape of pores: the thermoporometry. *Thermochim Acta.* 1977;21:59–88.
23. Morishige K, Yasunaga H, Denoyel R, Wernert V. Pore-blocking-controlled freezing of water in Cagelike Pores of KIT-5. *J Phys Chem C.* 2007;111:9488–95.
24. Janssen AH, Talsma H, van Steenberghe MJ, de Jong KP. Homogeneous nucleation of water in mesoporous zeolite cavities. *Langmuir.* 2004;20:41–5.
25. Pruppacher HRJ. A new look at homogeneous ice nucleation in supercooled water drops. *Atmos Sci.* 1995;52:1924–33.
26. Fajnor VŠ, Jesenák K. Differential thermal analysis of montmorillonite. *J Therm Anal.* 1996;46:489–93.
27. Kissinger HE. Reaction kinetics in differential thermal analysis. *Anal Chem.* 1957;29:1702–6.
28. Consolati G, Natali-Sora I, Pelosato R, Quasso F. Investigation of cation-exchanged montmorillonites by combined X-ray diffraction and positron annihilation lifetime spectroscopy. *J Appl Phys.* 2002;91:1928–32.
29. Stepanov SV, Zvezhinski DS, Duplâtre G, Byakov VM, Batskikh YY, Stepanov PS. Incorporation of the magnetic quenching effect into the blob model of Ps formation. Finite sized Ps in a potential well. *Mat Sci Forum.* 2011;666:109–14.